

# High-resolution structure of the *E. coli* RecQ helicase catalytic core

Douglas A. Bernstein, Morgan C. Zittel and James L. Keck<sup>1</sup>

Department of Biomolecular Chemistry, 550 Medical Science Center, 1300 University Avenue, University of Wisconsin Medical School, Madison, WI 53706-1532, USA

<sup>1</sup>Corresponding author  
e-mail: jlkeck@wisc.edu

**RecQ family helicases catalyze critical genome maintenance reactions in bacterial and eukaryotic cells, playing key roles in several DNA metabolic processes. Mutations in *recQ* genes are linked to genome instability and human disease. To define the physical basis of RecQ enzyme function, we have determined a 1.8 Å resolution crystal structure of the catalytic core of *Escherichia coli* RecQ in its unbound form and a 2.5 Å resolution structure of the core bound to the ATP analog ATP $\gamma$ S. The RecQ core comprises four conserved subdomains; two of these combine to form its helicase region, while the others form unexpected Zn<sup>2+</sup>-binding and winged-helix motifs. The structures reveal the molecular basis of missense mutations that cause Bloom's syndrome, a human RecQ-associated disease. Finally, based on findings from the structures, we propose a mechanism for RecQ activity that could explain its functional coordination with topoisomerase III.**

**Keywords:** helicase/RecQ/structure/winged helix/Zn<sup>2+</sup> binding

## Introduction

RecQ DNA helicases are ubiquitous enzymes in bacteria and eukaryotes that carry out important functions in genome biology (Cobb *et al.*, 2002; Wu and Hickson, 2002). Like other DNA helicases, RecQ proteins are ATP-dependent molecular motors that unwind double-stranded (ds) DNA. Members of the RecQ family differ from other helicases, however, in their unusual breadth of activities, including roles in DNA replication, recombination, and repair. With their central activities in genome maintenance, it is not surprising that mutation of many known *recQ* genes leads to genome instability and, in the case of three human *recQ* genes, to disease. Despite the importance of RecQ proteins, the structural basis of their function has remained poorly defined.

The founding RecQ family member was discovered in *Escherichia coli* where it functions in the RecF recombination pathway (Nakayama *et al.*, 1984; Umezu *et al.*, 1990). This pathway participates in homologous recombination and repair of ultraviolet light-induced DNA damage (Kowalczykowski *et al.*, 1994). RecQ and other proteins in the RecF pathway appear to catalyze reactions that help

repair replication forks that have stalled at sites of DNA damage (Courcelle *et al.*, 1997; Courcelle and Hanawalt, 1999; Courcelle *et al.*, 1999; 2003). In addition, *E. coli* RecQ helps suppress illegitimate recombination in cells (Hanada *et al.*, 1997). Although the precise cellular substrates on which RecQ proteins act remain a mystery, several reactions catalyzed by *E. coli* RecQ have been reconstituted *in vitro*, including ATP-dependent DNA unwinding (Umezu *et al.*, 1990), recombination initiation with RecA and single-stranded (ss) DNA binding protein (SSB) (Harmon and Kowalczykowski, 1998), and plasmid DNA catenation with topoisomerase III (Topo III) and SSB (Harmon *et al.*, 1999). Coordinated activities with recombinases and topoisomerases, as well as DNA unwinding functions, are conserved in a number of eukaryotic RecQ proteins (reviewed in Wu and Hickson, 2001), implying a functional homology among RecQ family members.

Three diseases (Bloom's, Werner's, and Rothmund–Thompson syndromes) can be attributed to mutations of human genes that encode homologs of *E. coli* RecQ (*BLM*, Ellis *et al.*, 1995; *WRN*, Yu *et al.*, 1996; *RECQ4*, Kitao *et al.*, 1999). While each of these syndromes has distinct clinical manifestations, they all share a predisposition to cancer. A common feature of these disorders is pronounced genomic instability, which is characterized by heightened levels of homologous recombination and/or chromosomal deletions (reviewed in Karow *et al.*, 2000). Several disease-linked nonsense and frame-shift mutations in *WRN*, *BLM*, and *RECQ4*, as well as all known *BLM* missense mutations associated with Bloom's syndrome, map to regions that are conserved across the RecQ family of enzymes.

Three regions conserved among bacterial and eukaryotic RecQ proteins have been identified by sequence analysis: helicase, RecQ-conserved (RecQ-Ct), and Helicase-and-RNaseD-C-terminal (HRDC) domains (Figure 1A; Morozov *et al.*, 1997). The helicase and RecQ-Ct regions are the best conserved regions among RecQ proteins, with some RecQs lacking an identifiable HRDC domain altogether. The RecQ family helicase region contains sequence motifs that are broadly conserved among DNA unwinding enzymes (Gorbalenya and Koonin, 1993). These motifs link the energy of nucleoside triphosphate binding and hydrolysis to DNA unwinding. The structure and function of the RecQ-Ct region is more poorly understood since it appears to be unique to RecQ proteins. However, evidence indicates that this region is essential for RecQ function. Two disease-causing *BLM* missense mutations map to the enzyme's RecQ-Ct region (Ellis *et al.*, 1995; Foucault *et al.*, 1997) and abolish *BLM* ATPase and helicase activities *in vitro* (Bahr *et al.*, 1998). Mutation and deletion analyses in the *Saccharomyces cerevisiae* RecQ homolog (Sgs1) have also shown that this

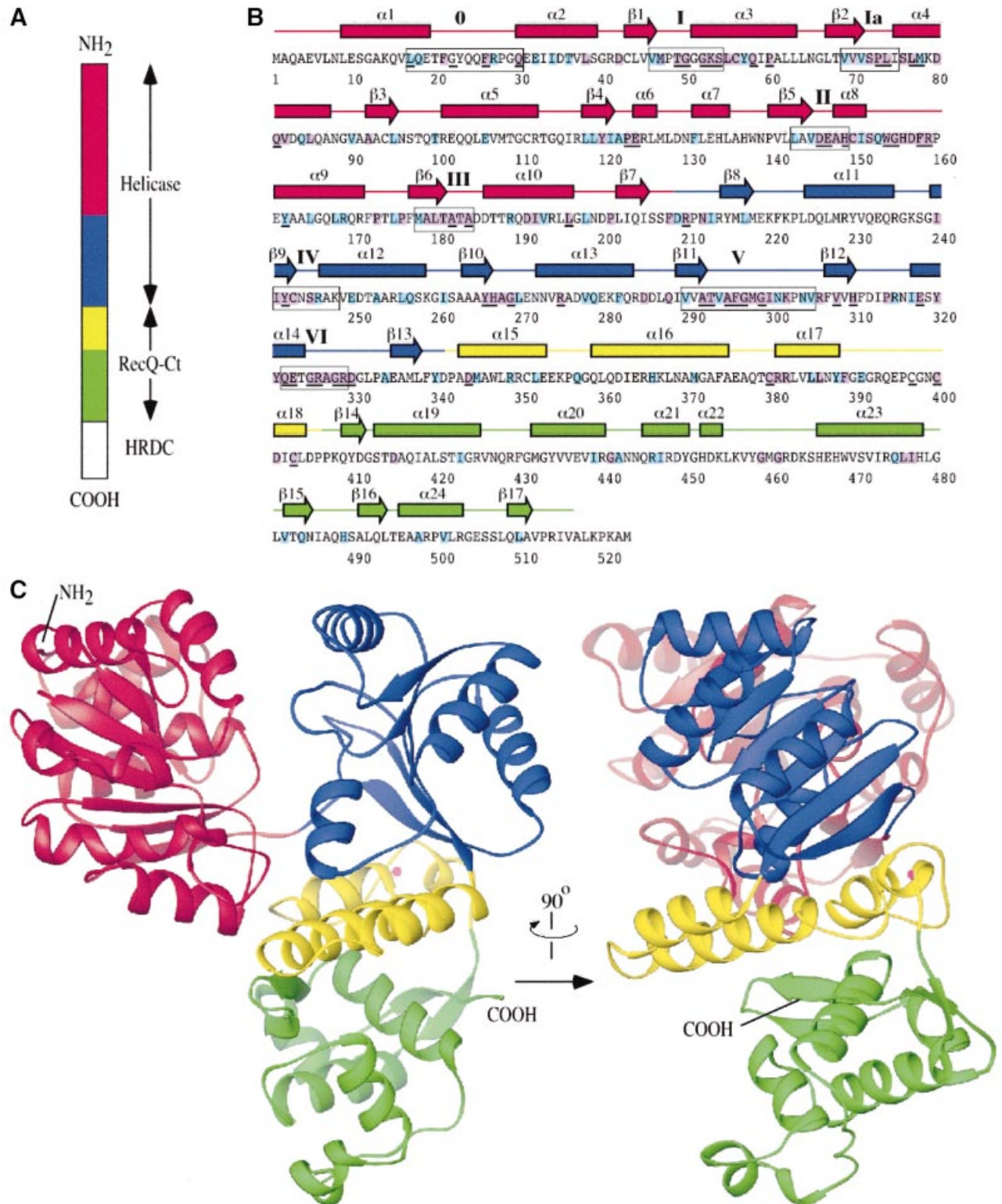


**Fig. 1.** Structure of the *E. coli* RecQ catalytic core. (A) Schematic diagram of *E. coli* RecQ. Three conserved regions, helicase, RecQ-conserved (RecQ-Ct), and Helicase-and-RNaseD-C-terminal (HRDC) (Morozov *et al.*, 1997), are labeled. The catalytic core of *E. coli* RecQ (RecQΔC) includes only the helicase and RecQ-Ct regions, and comprises four apparent subdomains in the structure: residues 1–208 in red, 209–340 in blue, 341–406 in yellow, and 407–516 in green. (B) Sequence and secondary structure of RecQΔC. Helices (boxes) and  $\beta$ -strands (arrows) are shown above the sequence and labeled sequentially. Color coding is the same as in (A). Conserved helicase motifs (motif 0, Bernstein and Keck, 2003; and motifs I–VI, Gorbalenya and Koonin, 1993) are labeled and enclosed in boxes. Residues that are invariant among 65 bacterial RecQ proteins are underlined, and residues that are invariant or highly conserved with a subset of eukaryotic RecQ proteins (human WRN, BLM, and *S. cerevisiae* Sgs1) are highlighted in purple or light-blue boxes, respectively. (C) Orthogonal views of a ribbon diagram of the crystal structure of RecQΔC, color-coded as in (A). A bound  $Zn^{2+}$  ion is shown as a magenta sphere.

region is essential for *in vivo* function (Mullen *et al.*, 2000; Onoda *et al.*, 2000; Ui *et al.*, 2001). Together, the helicase and RecQ-Ct regions form the core, conserved sequence that defines the RecQ family of enzymes.

Domain mapping experiments with *E.coli* RecQ have demonstrated that the conserved helicase and RecQ-Ct regions fold together to form a single 59 kDa structural domain (RecQ $\Delta$ C) (Bernstein and Keck, 2003). The isolated RecQ $\Delta$ C domain is active as a DNA-dependent ATPase and can unwind DNA with essentially the same specific activity as full-length *E.coli* RecQ, indicating that it is the catalytic core of the enzyme (Bernstein and Keck, 2003). The 9 kDa HRDC domain appears to modulate DNA binding activity of the catalytic core but is not necessary for enzyme function *in vitro* (Bernstein and Keck, 2003). Similarly, an *S.cerevisiae* Sgs1 variant that lacks its C-terminal HRDC domain can complement the increased DNA damage sensitivity phenotype of *sgs1* $\Delta$  cells (Mullen *et al.*, 2000; Mullen *et al.*, 2001), implying that the HRDC domain is dispensable for at least some activities *in vivo*. In addition, a recent study has shown that a catalytic core fragment of the human BLM protein that includes just its helicase and RecQ-Ct regions is active *in vitro* (Janscak *et al.*, 2003). These findings demonstrate that the evolutionarily conserved domain shared among RecQ proteins also forms the structural and catalytic core of the RecQ enzyme family.

Beyond low-resolution domain mapping, a number of other studies have revealed important structural features of RecQ helicases. First, sequence analysis places RecQ family members in the Superfamily 2 (SF2) group of enzymes (Gorbalenya and Koonin, 1993). While structurally similar to Superfamily 1 (SF1) enzymes, SF2 helicases are more similar to each other in sequence within their helicase domains than they are to SF1 enzymes. Secondly, the NMR structure of the *S.cerevisiae* Sgs1 HRDC domain has been determined (Liu *et al.*, 1999), revealing a domain that shares structural similarity with auxiliary DNA-binding domains in *E.coli* Rep and *Bacillus stearothermophilus* PcrA helicases (Subramanya *et al.*, 1996; Korolev *et al.*, 1997). Although this domain is not required for *E.coli* RecQ function and is not preserved in all RecQ family members, solution of this structure makes an important link to other well-studied helicases. Finally, a number of contradictory studies have investigated the active oligomeric state of RecQ helicases. Three findings indicate that RecQ proteins form oligomeric structures that may be important for their function: (i) *E.coli* RecQ hydrolyzes ATP with a Hill coefficient of 3 when unwinding DNA, implying that multiple ATPase sites interact during DNA strand separation (Harmon and Kowalczykowski, 2001); (ii) the human BLM protein forms homooligomeric ring structures (Karow *et al.*, 1999); and (iii) *Drosophila melanogaster* RecQ5 forms homooligomers (Kawasaki *et al.*, 2002). However, other recent findings may indicate that RecQ proteins can operate as monomers. These include a biochemical analysis of *E.coli* RecQ in centrifugation and kinetic experiments where it was concluded that the enzyme functions as a monomer (Xu *et al.*, 2003), and biochemical experiments with catalytically active recombinant fragments of the human BLM protein that no longer forms hexameric rings but instead exist as monomers

(Janscak *et al.*, 2003). Thus the question of the active oligomeric state of RecQ proteins remains unresolved.

To examine the physical basis of RecQ function, we have determined two high-resolution X-ray crystal structures of the conserved catalytic core of *E.coli* RecQ. The core domain comprises four apparent subdomains; two of the subdomains combine to form the helicase region and the remaining two join to form the RecQ-Ct region of RecQ. The RecQ-Ct subdomains include one that folds as a platform of helices that binds a Zn<sup>2+</sup> ion using four conserved cysteine residues and another that forms an unexpected winged-helix (WH) subdomain. The WH motif shares significant structural similarity with other DNA binding proteins, thus identifying a likely DNA binding site in *E.coli* RecQ. Based on the structures, we propose a mechanism of action that could explain the coordination of RecQ proteins with Topo III. Furthermore, our structures reveal the molecular basis of missense mutations that cause Bloom's syndrome. Together, these structures reveal the first high-resolution images of the enzymatic core conserved among RecQ family members.

## Results and discussion

### Structure determination of the RecQ $\Delta$ C domain

We first attempted to crystallize full-length *E.coli* RecQ protein, but extensive crystallization trials yielded no crystals. This result could have been due to flexibility that has been observed between the catalytic core and HRDC domains of *E.coli* RecQ (Bernstein and Keck, 2003) leading to structural heterogeneity that would hinder crystallization. Since we had characterized the catalytic core domain (RecQ $\Delta$ C) and found that it has essentially the same specific activities as full-length *E.coli* RecQ in ATPase and helicase assays (Bernstein and Keck, 2003), we subjected RecQ $\Delta$ C to crystallization trials as well and were able to crystallize it in a form that diffracted to 1.8 Å resolution (Table I). The crystal form contained one molecule per asymmetric unit. Crystals of selenomethionine-substituted RecQ $\Delta$ C were used to determine the structure of the domain using single-wavelength anomalous dispersion (SAD) phasing methods (Table I). The final refined model includes both the helicase and RecQ-Ct regions of the protein (residues 1 to 516 of RecQ $\Delta$ C, Figure 1B and C).

The RecQ $\Delta$ C structure reveals a modular, tri-lobed molecule that is comprised of four apparent structural subdomains (Figure 1C). The molecule is roughly 40 × 60 × 70 Å in size and forms a Y-shaped structure with major clefts apparent on its surface. The two N-terminal subdomains form distinct lobes of the molecule that combine to make the helicase region. The remaining two subdomains form the RecQ-Ct region, which is the third lobe of the molecule.

### Helicase region of RecQ

The two N-terminal subdomains of RecQ $\Delta$ C abut to form a deep cleft in the protein (Figure 1C). Conserved helicase sequence motifs (Gorbalenya and Koonin, 1993) line the cleft walls in an arrangement similar to that observed in other helicase structures (Caruthers and McKay, 2002) (Figure 2A). The RecQ $\Delta$ C helicase region is most similar in structure to helicase domains in other SF2 helicases,

**Table I.** Data collection, phasing, and refinement

Data collection	RecQΔC	ATPγS-bound RecQΔC	Phasing statistics	Refinement	RecQΔC	ATPγS-bound RecQΔC
Wavelength (Å)	0.9791	0.9000	Figure of merit	0.293	Resolution (Å)	20.0–1.8
Resolution (last shell) (Å)	74–1.8 (1.89–1.8)	21–2.5 (2.63–2.5)	(after density modification)	0.809	$R_{\text{work}}/R_{\text{free}}^b$	19.3/24.4
Measured reflections/unique	353 669/51 478	47 206/17 529			R.m.s.d. bond lengths (Å)	0.006
$R_{\text{sym}}^a$ (last shell) (%)	8.1 (44.2)	4.8 (13.3)			R.m.s.d. bond angles (°)	1.7
$I/\sigma$ (last shell)	16.3 (4.6)	12.8 (7.1)			PDB code	1OYW
Completeness (last shell) (%)	99.7 (99.7)	92.1 (92.1)				1OYY

<sup>a</sup> $R_{\text{sym}} = \sum_j |I_j - \langle I \rangle| / \sum_j I_j$ , where  $I_j$  is the intensity measurement for reflection  $j$  and  $\langle I \rangle$  is the mean intensity for multiply recorded reflections.

<sup>b</sup> $R_{\text{work, free}} = \sum |F_{\text{obs}}| - |F_{\text{calc}}| / |F_{\text{obs}}|$ , where the working and free  $R$ -factors are calculated using the working and free reflection sets, respectively. The free reflections (5% of the total) were held aside throughout refinement.

including three RNA helicases [*Methanococcus jannaschii* putative RNA helicase (Story *et al.*, 2001), *S. cerevisiae* eIF4a (Caruthers *et al.*, 2000), hepatitis C virus NS3 helicase (Yao *et al.*, 1997)], and *Thermotoga maritima* RecG DNA helicase (Singleton *et al.*, 2001), as well as the helicase domain in *Archaeoglobus fulgidus* reverse gyrase (Rodriguez and Stock, 2002). The RecQΔC structure also shares significant but lesser structural homology with SF1 DNA helicases and other ATP-binding proteins (see discussion below).

Based upon structural features of the RecQΔC helicase region that are conserved in other helicases, we hypothesized that ATP and ssDNA would bind to distinct sites within the helicase region, as indicated in Figure 2A. Consistent with this prediction, a second crystal structure of RecQΔC soaked in ATPγS, an ATP analog, and Mn<sup>2+</sup> showed clear  $F_o - F_c$  difference electron density for ATPγS and a metal ion in the predicted ATP binding site (Figure 2B). The adenine moiety is packed between Tyr23 and Arg27 side chains and hydrogen bonds are formed between the N6 and N7 atoms of the adenine and Gln30 of RecQ motif 0. This adenine binding mode likely explains the preference of ATP as a cofactor in *E. coli* RecQ reactions (Umezū *et al.*, 1990). Structural aspects of adenine binding by PcrA helicase (Subramanya *et al.*, 1996) are strikingly similar to those observed in RecQΔC. The ATPγS triphosphate is bound to RecQΔC by Lys53 and several backbone amides in motif I, and through a Mn<sup>2+</sup> ion that makes water-mediated contacts with Ser54 of motif I and Asp146 of motif II.

The presence of a ssDNA binding site between the RecQΔC helicase subdomains is predicted by its structural similarity to PcrA (Velankar *et al.*, 1999), Rep (Korolev *et al.*, 1997), and NS3 (Kim *et al.*, 1998) helicases solved with bound nucleic acid. In these structures, ssDNA binds to the two helicase lobes at a cleft that is on the opposite face from the ATP binding site. The interactions with ss nucleic acid are predominantly through either hydrophobic association with the DNA bases (Velankar *et al.*, 1999), ionic interactions with the substrate backbone (Kim *et al.*, 1998), or a combination of hydrophobic and ionic interactions with the nucleic acid substrate (Korolev *et al.*, 1997). However, an alternative DNA binding mechanism has recently been suggested based on the

*T. maritima* RecG helicase structure. In the RecG model, the helicase domain is proposed to bind to dsDNA and to act as a dsDNA translocase (Singleton *et al.*, 2001). Evidence supporting this model are that the path of dsDNA in the DNA-bound RecG structure extrapolates to the helicase domain (Singleton *et al.*, 2001) and that RecG's ATPase activity is significantly more sensitive to stimulation by dsDNA than ssDNA (Whitby and Lloyd, 1998). While the RecQΔC helicase region is structurally similar to that in RecG, *E. coli* RecQ's ATPase activity is ssDNA-dependent with only low levels of ATPase activity stimulated by dsDNA (Umezū *et al.*, 1990), and ssDNA-binding features similar to those found in PcrA are present in RecQΔC (see discussion below). Although we cannot rule out a RecG-type dsDNA translocase mechanism based on the structure of RecQΔC, the available evidence does not support this type of reaction. We currently favor a model for RecQΔC DNA binding where ssDNA binds between the two helicase subdomains as has been observed in PcrA, Rep, and NS3 helicases. Elucidation of the structural basis of RecQ DNA binding will require further experimental characterization.

### RecQ-Ct region of RecQ

The function of the RecQ-Ct region in RecQ-catalyzed reactions has not been well defined. RecQ-Ct sequences are not found in proteins outside of the RecQ family and previous functional characterization of this region in *S. cerevisiae* Sgs1 (Mullen *et al.*, 2000; Onoda *et al.*, 2000; Uj *et al.*, 2001), as well as in murine (Bahr *et al.*, 1998) and human (Janscak *et al.*, 2003) BLM proteins has been limited to mutational analyses. These studies indicate the importance of the RecQ-Ct region, but have not resolved its structure or function(s).

The RecQΔC structure shows that the RecQ-Ct region comprises two conserved subdomains. The first forms a platform of helices that is sandwiched between the helicase subdomains of RecQΔC and the rest of the RecQ-Ct region (Figures 1C and 3A). Inspection of the electron density map revealed that the side chains from four highly conserved cysteine residues at the ends of two of these helices were arrayed around a single intense electron density peak. This peak was modeled as a Zn<sup>2+</sup> ion since X-ray fluorescence experiments demonstrated

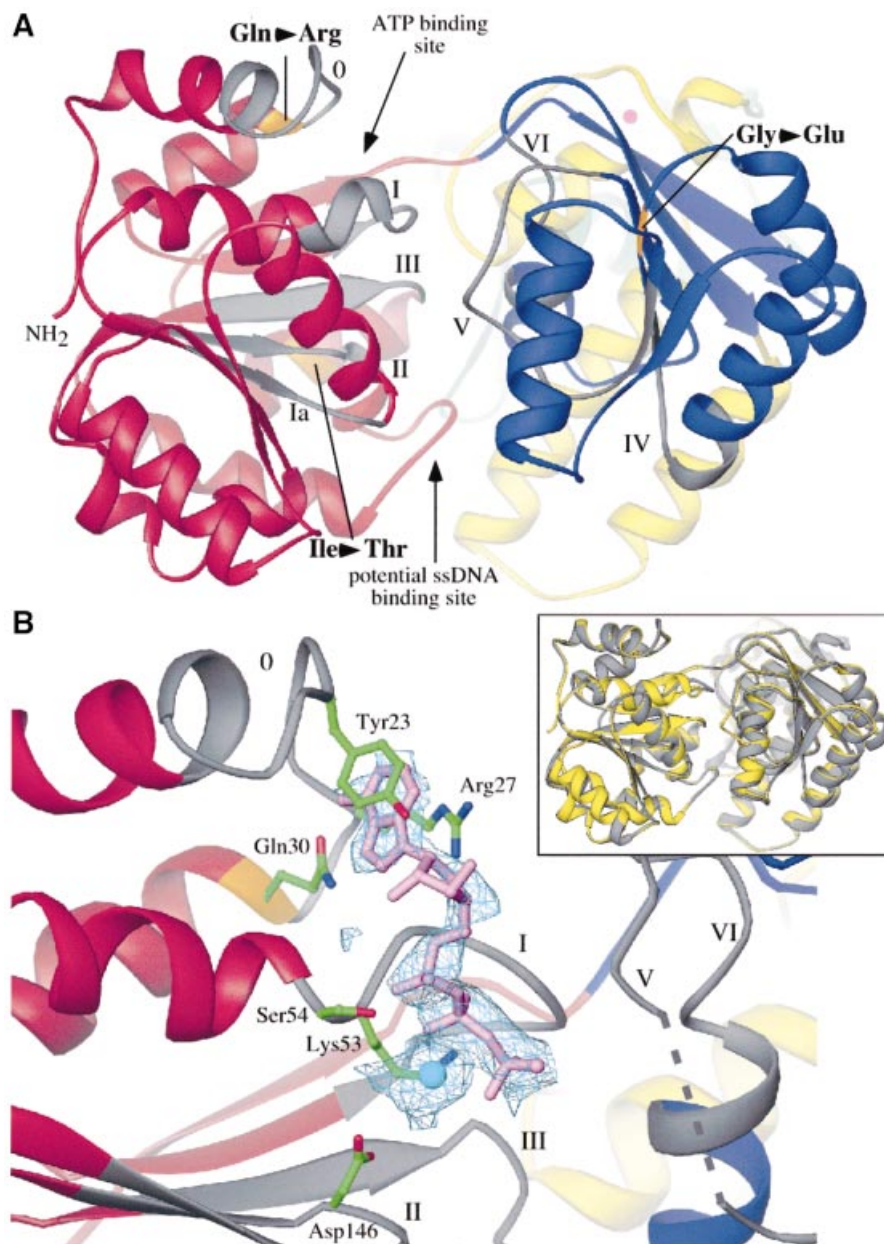


**Fig. 2.** Features of the helicase region of RecQ $\Delta$ C. **(A)** View into the cleft formed by the two helicase subdomains. Color coding is the same as Figure 1A, except that helicase motifs are labeled and colored in grey, and residues corresponding to known *BLM* missense mutations are labeled and colored in orange. Sites where nucleotide and ssDNA have been observed to bind in other helicase structures are indicated. **(B)** Structure of ATP $\gamma$ S/Mn $^{2+}$ -bound RecQ $\Delta$ C. (Inset) overlay of the apo- and ATP $\gamma$ S-bound RecQ $\Delta$ C structures in yellow and grey, respectively. A slight relative rotation of the second helicase lobe is seen in the structure with bound nucleotide. (Main panel)  $F_o - F_c$  difference electron density (light blue) is contoured at 1.5  $\sigma$ . Motif I is in an open conformation relative to its position in Figure 2A. The ATP $\gamma$ S (lavender) adenine moiety is sandwiched between Tyr23 and Arg27, and hydrogen bonds are formed between the N6 and N7 atoms of the adenine and the side chain of Gln30. The triphosphate is bound by interactions with Lys53 and backbone amides from motif I. A Mn $^{2+}$  ion (cyan) is bound by Ser54 from motif I and Asp146 from motif II. Helicase motif labels and color-coding are the same as in Figure 2A. Electron density was not observed for residues 296 to 299 (dashed line).

that Zn $^{2+}$  was present in the crystals in spite of its exclusion from any solutions used to purify or crystallize RecQ $\Delta$ C (data not shown). A second indication that this electron density peak identified a bound Zn $^{2+}$  ion came from biochemical analysis of *E. coli* RecQ (Figure 3B). In these experiments, the Zn $^{2+}$  content and the number of solvent-accessible thiol groups in *E. coli* RecQ were analyzed. The results indicated that *E. coli* RecQ copurifies with stoichiometric amounts of Zn $^{2+}$ . In addition, dialysis of *E. coli* RecQ against DTT and EDTA removed  $\sim 2/3$  of

the bound Zn $^{2+}$  and uncovered an additional 3–4 solvent-accessible thiol groups, consistent with the Zn $^{2+}$  binding site being comprised of 3–4 cysteines near the surface of RecQ. These biochemical data correlate well with the observed binding site in the structure.

Given the strong conservation of the Zn $^{2+}$ -binding site among RecQ proteins (Figure 1B), it is perhaps not surprising that functional analyses have shown this region to be important for RecQ function. *BLM* missense mutation sites in the RecQ-Ct region mutate codons for

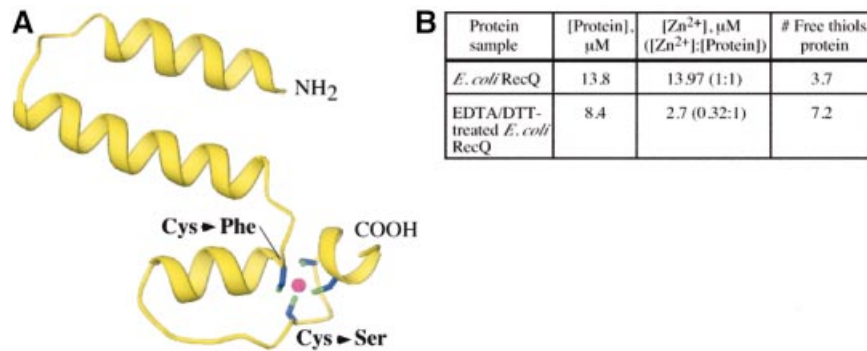


**Fig. 3.** Features of the Zn<sup>2+</sup>-binding subdomain in RecQΔC. **(A)** View of the Zn<sup>2+</sup>-binding subdomain (residues 341–406) extracted from the rest of RecQΔC. Four highly conserved cysteine residues (Cys380, Cys397, Cys400, Cys403) are arrayed around a Zn<sup>2+</sup> ion (magenta). Two *BLM* missense mutations alter individual cysteines in this array as labeled. The N- and C-terminal residues that connect to the helicase and WH subdomains, respectively, are labeled. **(B)** Biochemical evidence that full-length *E. coli* RecQ binds Zn<sup>2+</sup> in a site that includes 3–4 cysteine residues. [Zn<sup>2+</sup>] and [thiol]<sub>free</sub> were determined for *E. coli* RecQ and *E. coli* RecQ that was dialyzed against 10 mM EDTA, 1 mM DTT to extract bound Zn<sup>2+</sup>.

cysteine residues in BLM protein that are analogous to residues 380 or 397 in *E. coli* RecQ (Ellis *et al.*, 1995; Foucault *et al.*, 1997; see discussion below). In addition, mutated *S. cerevisiae* *SGS1* genes fail to complement the DNA-damage sensitivity and hyperrecombination phenotypes in an *sgs1Δ* strain when any of the analogous Zn<sup>2+</sup>-binding site cysteine residues have been altered (Onoda *et al.*, 2000; Ui *et al.*, 2001). Finally, a number of point mutations in residues analogous to RecQΔC Zn<sup>2+</sup>-liganding cysteines in either the human BLM protein catalytic core (Janscak *et al.*, 2003) or in *E. coli* RecQ (M.C.Zittel and J.L.Keck, unpublished observation) result in variants that are difficult to purify due perhaps to rapid proteolysis, indicating that Zn<sup>2+</sup> binding to this region may stabilize the protein. The RecQ Zn<sup>2+</sup>-binding motif is unlike previously observed zinc finger folds (Krishna *et al.*, 2003), and does not have substantial structural similarity with any other known proteins. Future experiments will therefore be needed to determine its specific function in RecQ. Potential functions could include thermodynamic stabilization of the protein and/or acting as a DNA or protein binding site, all of which have been observed for Zn<sup>2+</sup>-binding domains in other proteins (Berg and Shi, 1996).

The second RecQ-Ct subdomain forms a specialized helix–turn–helix fold called a WH subdomain, which has been found to act as a DNA-binding motif in many proteins (Gajiwala and Burley, 2000; Figure 4A). The RecQ WH fold is structurally homologous to WH domains found in reverse gyrase (Rodriguez and Stock, 2002) and other type-IA topoisomerases (Lima *et al.*, 1994; Mondragon and DiGate, 1999) as well as to several other DNA binding proteins, including the *E. coli* catabolite gene activator protein (CAP) (Schultz *et al.*, 1991). The intersection of the RecQ WH and Zn<sup>2+</sup>-binding helical subdomains creates a large cleft on the surface of the protein. Several features of this cleft suggest that it can serve as a binding site for dsDNA: (i) the expected dsDNA binding face of the WH fold, including the putative DNA binding ‘recognition helix’, forms an exposed wall of the cleft; (ii) several residues that mediate WH/DNA phosphate interactions in other proteins are conserved in the RecQ WH domain (Figure 4B); and (iii) superposition of the dsDNA from the CAP/DNA co-crystal structure onto

the WH RecQ fold demonstrates that the cleft could accommodate dsDNA without needing to significantly alter the structure of the RecQ-Ct region (Figure 4C). In support of this dsDNA binding model, we have found that a recombinant HRDC domain fragment from *E. coli* RecQ, which would be localized near the putative dsDNA binding site on the RecQ-Ct region in the full-length protein, has a strong binding preference for dsDNA over ssDNA (D.A.Bernstein and J.L.Keck, unpublished observation). dsDNA binding by the HRDC domain could serve as a clamp to stabilize dsDNA binding to the catalytic core. This model is consistent with previous observations of different DNA binding stabilities between *E. coli* RecQ and RecQΔC (Bernstein and Keck, 2003).

#### Comparison of RecQΔC to SF1 and SF2 helicases

Sequence analysis of RecQ proteins have placed them among the SF2 group of helicases (Gorbalenya and Koonin, 1993), which includes several members with known structures. Consistent with its sequence alignment with other SF2 enzymes, the RecQΔC structure is more closely related to other SF2 family members in structure than to SF1 enzymes. For example, the two RecQΔC helicase lobes align better with hepatitis C virus NS3 helicase (Yao *et al.*, 1997), an SF2 enzyme (DALI Z-score = 14.9 for 224 Cα atoms) than with PcrA helicase (Subramanya *et al.*, 1996), the SF1 enzyme that is most structurally similar to RecQΔC (Z-score = 9.8 for 244 Cα atoms) (Holm and Sander, 1993) (Figure 5). Nevertheless, RecQΔC’s similarity with PcrA is still informative. As mentioned above, RecQΔC’s mode of ATP binding is quite similar to that seen in PcrA. In addition, a patch of conserved aromatic and charged residues in RecQΔC (residues 156–159, C-terminal to helicase motif II in RecQΔC) map to the same relative surface location as similar residues in PcrA that are used in DNA binding (residues 257–260, C-terminal to motif III in PcrA) (Velankar *et al.*, 1999). This structural conservation between RecQΔC and PcrA could indicate that the enzymes use conserved mechanisms of DNA binding and unwinding. RecQΔC primarily differs from other helicases by its novel accessory elements in the RecQ-Ct

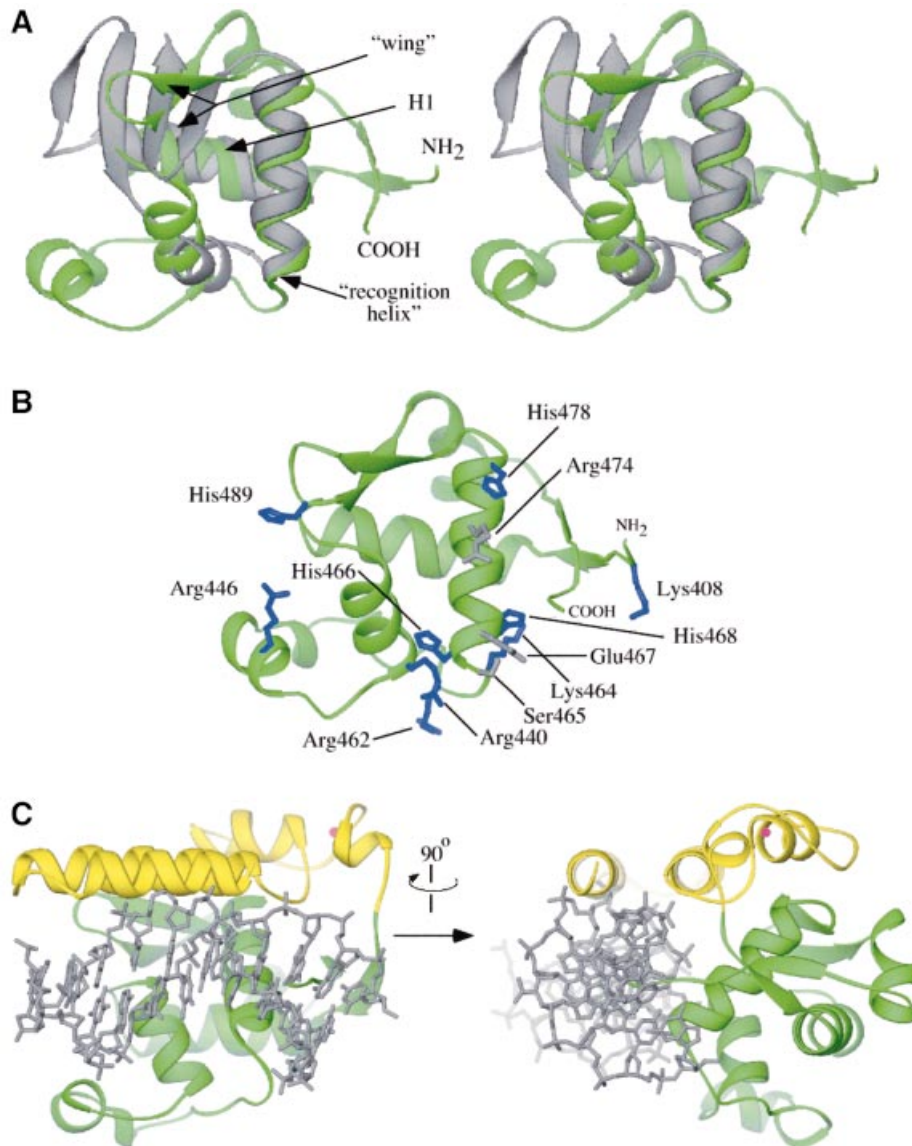


**Fig. 4.** Features of the WH subdomain in RecQ $\Delta$ C. (A) Stereo diagram of the superposition of the WH subdomain extracted from the RecQ $\Delta$ C structure (green, residues 407–516) with the DNA binding WH domain of CAP (Schultz *et al.*, 1991) (grey). The two major helices of the fold (H1 and recognition helix) and the wing elements are labeled. The N-terminal residue of the RecQ $\Delta$ C WH fold, which connects to the Zn<sup>2+</sup> binding region, and C-terminal residue are labeled. (B) Potential DNA binding residues in the RecQ $\Delta$ C WH subdomain. Residues that are structurally conserved with DNA binding residues in CAP (Schultz *et al.*, 1991) are shown in grey and other residues with positive charge potential on the same putative DNA binding face are shown in blue. (C) Orthogonal views of a model of dsDNA binding to the RecQ-Ct region of RecQ. dsDNA from the CAP/DNA complex structure (grey) (Schultz *et al.*, 1991) is overlaid onto the RecQ-Ct region. A minor opening of the helical Zn<sup>2+</sup>-binding region relative to the WH region would create a cleft sufficiently wide for dsDNA binding.

domain (Figure 5). These features will most likely prove critical to the specialized functions of RecQ proteins.

#### **Structural basis of Bloom's syndrome missense mutations**

Several recessive mutations in the human *BLM*, *WRN*, and *RECQ4* genes are known to cause Bloom's, Werner's, and Rothmund–Thompson syndromes, respectively. Many of the mutations in *BLM* and all known disease-associated alleles in *WRN* and *RECQ4* are nonsense or frame-shift mutations that would express truncated versions of the proteins (Kitao *et al.*, 1999). In *WRN* protein, these mutations lead to mislocalization in the cell due to failure to express the C-terminal nuclear localization sequence

(Matsumoto *et al.*, 1997). A similar rationale might also explain the phenotypes of *BLM* nonsense alleles (Matsumoto *et al.*, 1998). In addition to nonsense and frame-shift mutations, seven missense mutations in *BLM* leading to single amino acid changes in the protein are known to cause Bloom's syndrome (Ellis *et al.*, 1995; Foucault *et al.*, 1997; Barakat *et al.*, 2000; Rong *et al.*, 2000). Three of these mutations have been shown to inactivate the murine *BLM* protein *in vitro* (Bahr *et al.*, 1998), implying that the missense mutations cause disease as a result of enzymatic failure. All seven known disease-linked *BLM* missense mutations map to the RecQ family catalytic core domain, with five of them occurring in residues identically conserved within the *E.coli* RecQ

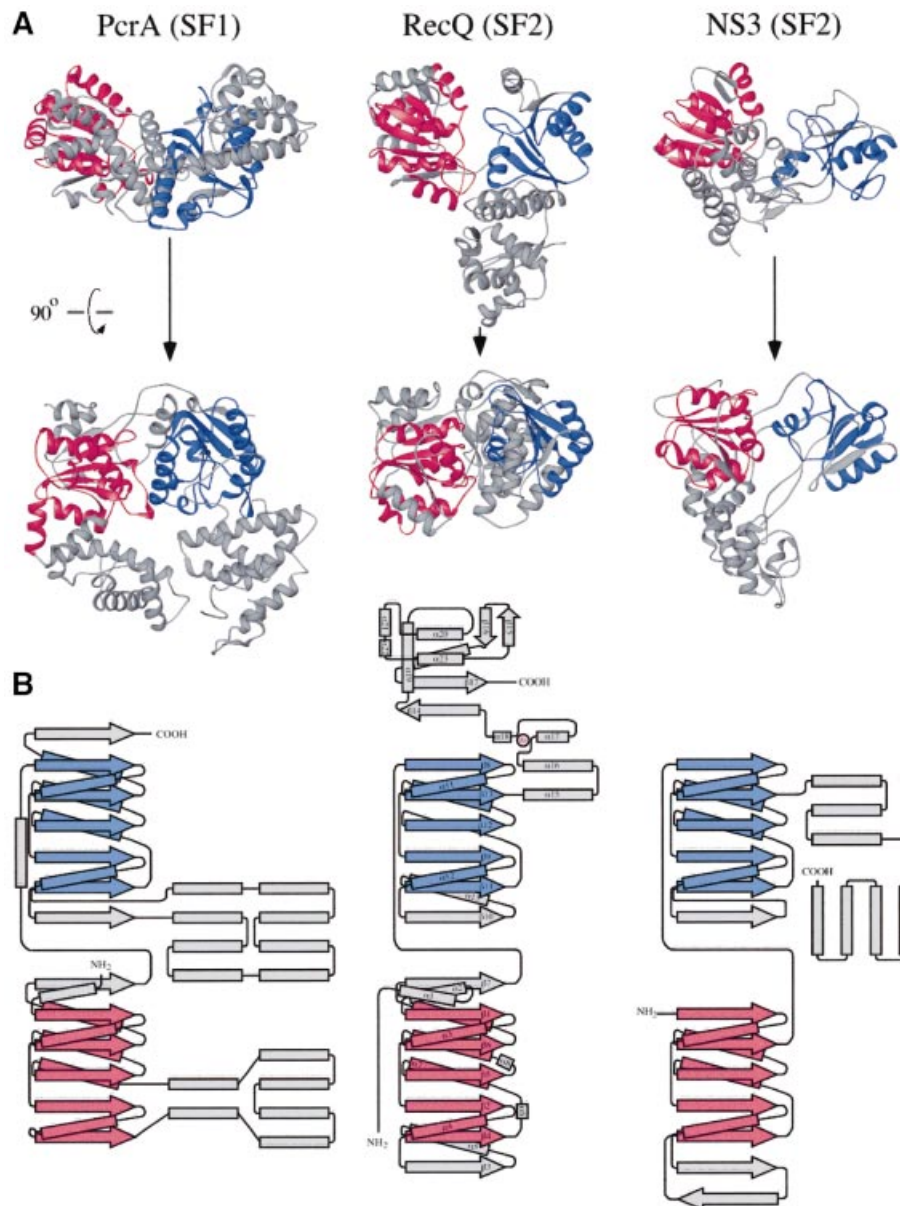


**Fig. 5.** Structural comparison of RecQ $\Delta$ C to representative helicases belonging to the SF1 and SF2 helicase superfamilies. (A) Structures of PcrA (Subramanya *et al.*, 1996) and NS3 (Yao *et al.*, 1997), SF1 and SF2 helicases, respectively, were superimposed on RecQ $\Delta$ C using the structurally related C $\alpha$  atoms in their N-terminal most helicase subdomains (in red) and then translated to allow visual comparison. Red and blue colors mark the conserved RecA-like folds found in the helicase subdomains of each protein, while grey coloration indicates sequences outside of the RecA fold. An orthogonal view is shown of each protein below the top row. (B) Topology diagrams of PcrA, RecQ $\Delta$ C and NS3. Colors are shown as in (A), with RecQ $\Delta$ C's Zn<sup>2+</sup> in magenta. Helices and  $\beta$ -strands in RecQ $\Delta$ C are labeled as in Figure 1B. Diagrams of PcrA and NS3 were adapted from Caruthers and McKay (2002).

sequence. Given the ability of a catalytically active fragment of human BLM protein to complement mutation of the *recQ* gene in *E. coli* (Janscak *et al.*, 2003), the RecQ $\Delta$ C structure provides an excellent model for rationalizing the biophysical basis underlying known *BLM* missense mutations.

Five of the seven *BLM* missense mutations map to the helicase region of the protein: Gln672Arg, Ile841Thr, Cys878Arg, Gly891Glu, and Cys901Tyr (Ellis *et al.*, 1995; Barakat *et al.*, 2000; Rong *et al.*, 2000). Three of these positions are conserved in RecQ $\Delta$ C (Gln30, Ile192 and Gly239), whereas the two cysteines are poorly

conserved among RecQ helicases. The RecQ $\Delta$ C structures reveal plausible effects of these missense mutations that could impair enzyme function. The first mutation, Gln $\rightarrow$ Arg, would likely diminish ATP binding to RecQ, since the equivalent Gln in RecQ $\Delta$ C (Gln30) contacts the adenine moiety of the nucleotide cofactor directly through hydrogen bonds (Figure 2B). Mutation of this conserved Gln results in loss of ATPase and helicase activity in the murine BLM protein (Bahr *et al.*, 1998), consistent with its observed role in ATP binding. The other *BLM* helicase mutations are likely to affect protein folding or stability (Figure 2A). Both the Ile $\rightarrow$ Thr and Gly $\rightarrow$ Glu mutations



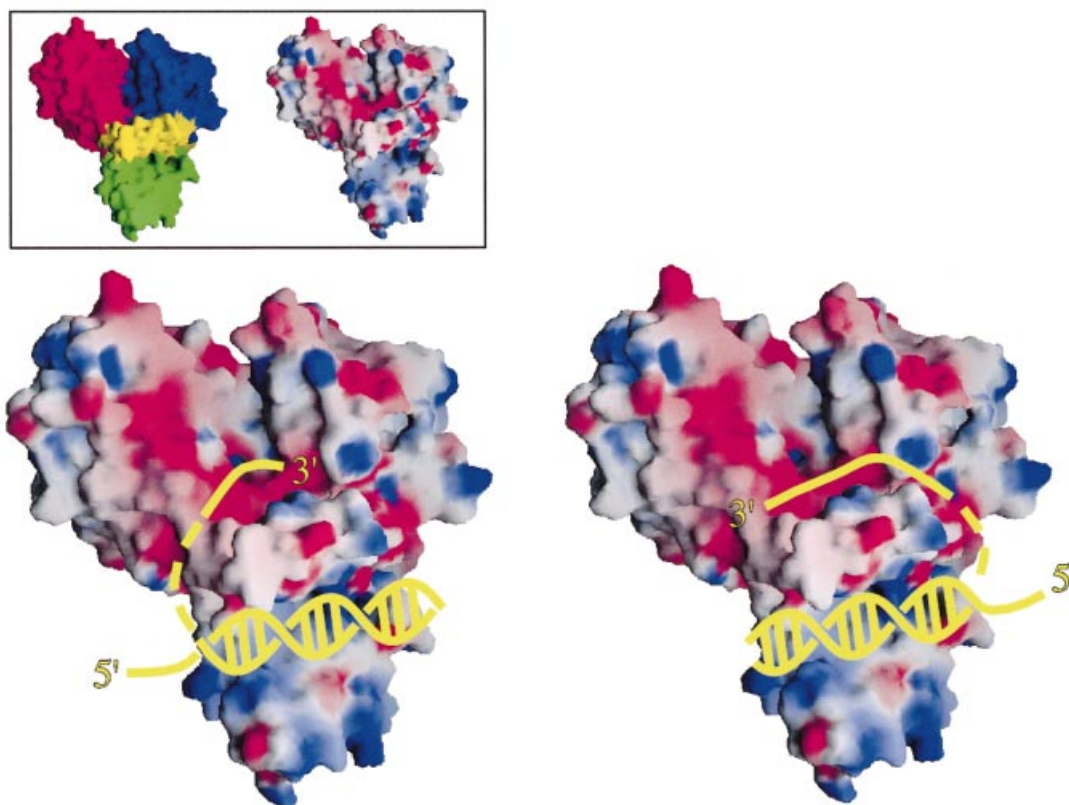


**Fig. 6.** Models for DNA binding to *E. coli* RecQ $\Delta$ C. Surface representations of *E. coli* RecQ $\Delta$ C are shown (color-coded as in Figure 1, inset left) bound to cartoon diagrams of a partially unwound DNA molecule in two possible orientations (yellow). The RecQ $\Delta$ C surface is colored by its electrostatic surface potential (inset right and main panel) at + or -6 k<sub>B</sub>T/e for positive (blue) or negative (red) charge potential using the program GRASP (Nicholls *et al.*, 1991). Since *E. coli* RecQ may unwind DNA as an oligomer (Harmon and Kowalczykowski, 2001), it is not clear whether ssDNA bound by the helicase region would come from dsDNA bound by the same protomer or another protomer in the oligomer during unwinding. As such, the connection linking the dsDNA to the 3' ssDNA is shown as a dashed line. In addition, relative subdomain orientations could change in the DNA-bound form.

introduce polar side chains into the hydrophobic core of the helicase subdomains, which would likely destabilize folded BLM protein and could inactivate the enzyme.

The two remaining disease-linked *BLM* missense mutations, Cys1036Phe and Cys1055Ser (Ellis *et al.*, 1995; Foucault *et al.*, 1997), alter residues analogous to two that directly bind Zn<sup>2+</sup> in RecQ $\Delta$ C (Figure 3A). These mutations introduce either a large hydrophobic group (Phe) or a poor Zn<sup>2+</sup> ligand (Ser) into the structure. Either mutation could reduce Zn<sup>2+</sup> binding, thus altering the structure of this region of the enzyme. Previous studies have shown that these mutations inactivate the murine BLM protein *in vitro* (Bahr *et al.*, 1998), thus highlighting the importance of the Zn<sup>2+</sup>-binding region to proper RecQ family function.

#### **Model for RecQ catalytic function**

Using structural information from the RecQ $\Delta$ C structures, we have constructed a general model for RecQ activity. Two likely DNA binding sites are present in RecQ $\Delta$ C: a ssDNA binding site that is similar to those observed in other helicases (Figure 2A), and a putative dsDNA binding site in the RecQ-Ct region (Figure 4C). An arrangement in which the RecQ-Ct region binds dsDNA and ssDNA is bound between the helicase subdomains therefore seems plausible in RecQ (Figure 6). We predict that the 3' ssDNA

end of unwound DNA would be bound to the helicase region, since RecQ proteins unwind dsDNA in a 3'→5' direction (Umezu *et al.*, 1990). RecQ helicase activity would produce 3' and 5' ss segments of unwound DNA as potential substrates for enzymatic partners of RecQ that require ssDNA, such as RecA (Harmon and Kowalczykowski, 1998) or Topo III (Harmon *et al.*, 1999). Moreover, conserved surface features of RecQ, such as the Zn<sup>2+</sup>-binding subdomain, could provide protein-protein interaction sites or additional DNA binding surfaces. Since our structure is of a monomer of RecQ $\Delta$ C, but full-length *E. coli* RecQ might function as an oligomer in DNA unwinding (Harmon and Kowalczykowski, 2001), it is not clear whether the ds and ss portions of DNA being unwound by RecQ would bind to the same or different protomers in a RecQ oligomer. In addition, DNA binding could alter the domain arrangement in RecQ $\Delta$ C as has been observed for PcrA helicase (Velankar *et al.*, 1999). Future studies will be required to investigate the structural dynamics associated with DNA binding in *E. coli* RecQ.

#### **Insights into the nature of RecQ functions with topoisomerase III**

Important functional interactions between RecQ and Topo III homologs have been reported for many organisms

(reviewed in Wu and Hickson, 2001; Oakley and Hickson, 2002; Wang, 2002), but a model explaining their joint activity has been hampered by the lack of structural information on RecQ. DNA unwinding by a helicase such as RecQ creates domains of (+) and (–) supercoiled DNA (Liu and Wang, 1987; Peter *et al.*, 1998). The ssDNA product from DNA unwinding is a substrate for Topo III, which selectively relaxes (–) supercoiled DNA (DiGate and Marians, 1988). Thus, the net product of RecQ/Topo III activities would likely be (+) supercoiled DNA. As previously proposed, this reaction would constitute a ‘reverse gyrase’ activity (Gangloff *et al.*, 1994). Reverse gyrases have thus far been found only in thermophilic eubacteria and archaea, and they contain both helicase and type-IA topoisomerase domains (reviewed in Champoux, 2001). The RecQAC structure reveals an important clue as to how RecQ might have evolved to support a reverse gyrase-like activity, since its major subdomains are structurally homologous to the helicase and WH regions of *A. fulgidis* reverse gyrase (Rodriguez and Stock, 2002). In addition, RecQAC has a Zn<sup>2+</sup>-binding domain, an element that is lacking in bacterial and yeast Topo III homologs but present in other type-IA topoisomerases, such as reverse gyrase (Champoux, 2001). We propose that RecQ and Topo III could function together in a manner similar to reverse gyrase using functional domains supplied by both proteins. Interaction between RecQ and Topo III could position Topo III in close proximity to ssDNA produced by the RecQ helicase domain, thereby providing Topo III with substrate. The joint action of RecQ and Topo III may not rely on processive DNA unwinding but could involve a local melting of DNA by RecQ and relaxation by Topo III. This reverse gyrase-like activity could be an important common step in many RecQ-mediated DNA remodeling functions in cells.

The structures of the catalytic core of *E. coli* RecQ presented here yield insights into the molecular origins of human diseases that stem from mutations of *recQ* genes and offer new clues that will help elucidate the biochemical mechanisms used by the RecQ family of DNA helicases. These findings help pave the way for uncovering the precise functions of RecQ proteins in cellular genome maintenance reactions.

## Materials and methods

### Protein expression and purification

T7-overexpression plasmids encoding either full-length *E. coli* RecQ or RecQAC (residues 1–523) preceded by a His<sub>6</sub> affinity-purification tag were constructed, and the proteins were overexpressed and purified as previously described (Bernstein and Keck, 2003). Selenomethionine-incorporated RecQAC was expressed as described in Van Duyne *et al.* (1993), and was purified as for the unsubstituted protein, except that 0.8 mM Tri(2-carboxyethyl) phosphine hydrochloride (TCEP) was added to all buffers, the NaCl concentration of all buffers was adjusted to 500 mM, and the ion exchange purification step was eliminated from the purification procedure.

### Crystallization of RecQAC

Native or selenomethionine-incorporated RecQAC was dialyzed against buffer containing 10 mM Tris pH 8.0 and 500 mM ammonium acetate. Crystals of native RecQAC were grown by hanging drop vapor diffusion by mixing 0.9  $\mu$ l of 20 mg/mL protein, 0.2  $\mu$ l of 100 mM MnCl<sub>2</sub>, and 0.9  $\mu$ l of well solution [0.5% polyethylene glycol (PEG) 1000, 2–4% PEG400, 50 mM MES pH 6.5, 50 mM ammonium sulfate] and equilibrating at room temperature for several days. Crystals measuring

~200  $\mu$ m  $\times$  ~100  $\mu$ m  $\times$  ~50  $\mu$ m of symmetry  $P2_1$  with unit cell length  $a = 65$ ,  $b = 54$  and  $c = 78$  Å,  $\beta = 110.7^\circ$  were formed. This crystal form has one molecule of RecQAC per asymmetric unit. Isomorphous selenomethionine-incorporated RecQAC crystals were grown by microseeding with native crystals. Crystals were stabilized by transferring into a cryoprotectant solution (3% PEG1000, 50 mM HEPES pH 7.5, 10 mM MnCl<sub>2</sub>, 25% ethylene glycol) and frozen in liquid nitrogen. Crystals with ATP $\gamma$ S bound were obtained by soaking native RecQAC crystals in 2.5% PEG1000, 50 mM HEPES pH 7.5, 10 mM ATP $\gamma$ S, 5 mM MgCl<sub>2</sub>, for 3 days at room temperature, and were then transferred to cryoprotectant buffer and frozen in liquid nitrogen.

### SAD phasing and model refinement

Selenomethionine-incorporated crystals were solved by SAD phasing to 1.8 Å (Table I). Data were indexed and scaled with MOSFLM (Leslie, 1992) and SCALA (Kabsch, 1988). Selenium sites were determined with SHELX (Schneider and Sheldrick, 2002) and refined with MLPHARE (Otwinowski, 1991). Solvent flattening with DM (Cowtan, 1994) resulted in interpretable experimental electron density maps for model building. Over 90% of the model was built automatically using ARP/wARP (Lamzin and Wilson, 1993), with the remainder built manually using the program O (Jones *et al.*, 1991) and improved by rounds of refinement with REFMAC/ARP (Lamzin and Wilson, 1993; Murshudov *et al.*, 1997) and manual rebuilding. The final model contains residues 1–516. No bond angles for this model fall into disallowed regions of Ramachandrian space.

### Molecular replacement solution of nucleotide-bound RecQAC

The ATP $\gamma$ S/Mn<sup>2+</sup>-bound RecQAC structure was solved by molecular replacement using AMORE (Navaza, 2001) with the unbound RecQAC structure as a search model. The molecular replacement solution was refined with REFMAC/ARP (Lamzin and Wilson, 1993; Murshudov *et al.*, 1997) and by manually rebuilding the model using O (Jones *et al.*, 1991). Since the nucleotide soaking solution contained 5 mM MgCl<sub>2</sub> but the cryoprotectant used to stabilize the crystals prior to freezing included 10 mM MnCl<sub>2</sub>, the identity of the bound metal was ambiguous. We therefore attempted to refine the structure with either a Mg<sup>2+</sup> or a Mn<sup>2+</sup> ion in the binding site. Placing a Mn<sup>2+</sup> ion in the site satisfied the observed scattering, whereas using a Mg<sup>2+</sup> ion left substantial positive difference electron density and refined the atomic *B*-factor of the metal to an unrealistically low value. Therefore, the metal was modeled as a Mn<sup>2+</sup> ion. *E. coli* RecQ has essentially the same level of ATPase activity using either Mg<sup>2+</sup> or Mn<sup>2+</sup> as a cofactor (Umezū *et al.*, 1990). The final model contains residues 1–516 excluding residues 296–299 for which electron density was not observed. No bond angles for this model fall into disallowed regions of Ramachandrian space.

### Quantitation of Zn<sup>2+</sup> bound to *E. coli* RecQ

The Zn<sup>2+</sup> content of purified full-length *E. coli* RecQ was measured using 4-(2-pyridylazo)resorcinol (PAR), a reporter dye that absorbs light at 490 nm when bound to Zn<sup>2+</sup> (Hunt *et al.*, 1984). Zn<sup>2+</sup> was extracted from a sample of purified RecQ by dialysis against 20 mM Tris pH 8.0, 300 mM NaCl, 10% glycerol, 10 mM EDTA, 1 mM DTT, at 4°C overnight. One hundred microliters of untreated RecQ or Zn<sup>2+</sup>-extracted RecQ (in 10% glycerol, 300 mM NaCl, 20 mM Tris–HCl pH 8.0) was incubated with 60  $\mu$ g Proteinase K at 37°C for 1 h. Two microliters of 5 mM PAR was then added to each sample and their absorbances at 490 nm were measured and compared to a standard curve of ZnCl<sub>2</sub> samples at a range of concentrations using an identical sample preparation procedure as described above, but omitting RecQ. RecQ concentrations were determined as in Bernstein and Keck, (2003).

### Quantitation of free thiol groups in *E. coli* RecQ

[thiols<sub>free</sub>] in *E. coli* RecQ and Zn<sup>2+</sup>-extracted RecQ were determined by measuring the absorbance at 412 nm following reaction of 5,5'-dithiobis (2-nitrobenzoic acid) (DTNB) with thiols in the protein as described in Riddles *et al.* (1983). Ten microliters of 10 mM DTNB (in 0.1 M NaPhosphate pH 8.0) was added to 10  $\mu$ l of untreated or Zn<sup>2+</sup>-extracted *E. coli* RecQ (in 10% glycerol, 300 mM NaCl, 20 mM Tris–HCl pH 8.0) and diluted into 300  $\mu$ l of 0.1 M NaPhosphate pH 8.0. Samples were incubated at room temperature for 1 h and their absorbances at 412 nm were measured. These values were converted to [thiols<sub>free</sub>] as described in Riddles *et al.* (1983).

**Accession numbers**

Model coordinates and structure factors have been deposited in the Protein Data Bank under accession codes 1OYW and 1OYY.

**Acknowledgements**

We thank James Holton (Advanced Light Source beamline 8.3.1) and the Advanced Photon Source beamline staff (BioCARS beamline 14-BMC) for assistance in data collection, and Bruker AXS for generous use of their instrumentation. R.J.Bennett, J.M.Berger, D.A.Brow, E.A.Craig, J.E.Dahlberg and E.Shor contributed helpful discussions. This work was supported by a grant from the NIH to J.L.K. (GM068061), start-up funds from the University of Wisconsin, and a grant from the University of Wisconsin Medical School under the Howard Hughes Medical Institute Research Resources Program for Medical Schools. D.A.B. was supported in part by an NIH training grant in Molecular Biophysics (GM08293).

**References**

- Bahr,A., De Graeve,F., Keding,C. and Chatton,B. (1998) Point mutations causing Bloom's syndrome abolish ATPase and DNA helicase activities of the BLM protein. *Oncogene*, **17**, 2565–2571.
- Barakat,A., Ababou,M., Onclercq,R., Dutertre,S., Chadli,E., Hda,N., Benslimane,A. and Amor-Gueret,M. (2000) Identification of a novel BLM missense mutation (2706T>C) in a Moroccan patient with Bloom's syndrome. *Hum. Mutat.*, **15**, 584–585.
- Berg,J.M. and Shi,Y. (1996) The galvanization of biology: a growing appreciation for the roles of zinc. *Science*, **271**, 1081–1085.
- Bernstein,D.A. and Keck,J.L. (2003) Domain mapping of *Escherichia coli* RecQ defines the roles of conserved amino- and carboxyl-terminal regions in the RecQ family. *Nucleic Acids Res.*, **31**, 2778–2785.
- Caruthers,J.M., Johnson,E.R. and McKay,D.B. (2000) Crystal structure of yeast initiation factor 4A, a DEAD-box RNA helicase. *Proc. Natl Acad. Sci. USA*, **97**, 13080–13085.
- Caruthers,J.M. and McKay,D.B. (2002) Helicase structure and mechanism. *Curr. Opin. Struct. Biol.*, **12**, 123–133.
- Champoux,J.J. (2001) DNA topoisomerases: structure, function and mechanism. *Annu. Rev. Biochem.*, **70**, 369–413.
- Cobb,J.A., Bjergbaek,L. and Gasser,S.M. (2002) RecQ helicases: at the heart of genetic stability. *FEBS Lett.*, **529**, 43–48.
- Courcelle,J., Carswell-Crumpton,C. and Hanawalt,P.C. (1997) recF and recR are required for the resumption of replication at DNA replication forks in *Escherichia coli*. *Proc. Natl Acad. Sci. USA*, **94**, 3714–3719.
- Courcelle,J., Crowley,D.J. and Hanawalt,P.C. (1999) Recovery of DNA replication in UV-irradiated *Escherichia coli* requires both excision repair and recF protein function. *J. Bacteriol.*, **181**, 916–922.
- Courcelle,J., Donaldson,J.R., Chow,K.H. and Courcelle,C.T. (2003) DNA damage-induced replication fork regression and processing in *Escherichia coli*. *Science*, **299**, 1064–1067.
- Courcelle,J. and Hanawalt,P.C. (1999) RecQ and RecJ process blocked replication forks prior to the resumption of replication in UV-irradiated *Escherichia coli*. *Mol. Gen. Genet.*, **262**, 543–551.
- Cowtan,K. (1994) Joint CCP4 ESF-EACBM Newsletter. *Protein Crystallogr.*, **31**, 34.
- DiGate,R.J. and Marians,K.J. (1988) Identification of a potent decatenating enzyme from *Escherichia coli*. *J. Biol. Chem.*, **263**, 13366–13373.
- Ellis,N.A., Groden,J., Ye,T.Z., Straughen,J., Lennon,D.J., Ciocci,S., Proytcheva,M. and German,J. (1995) The Bloom's syndrome gene product is homologous to RecQ helicases. *Cell*, **83**, 655–666.
- Foucault,F., Vaury,C., Barakat,A., Thibout,D., Planchon,P., Jaulin,C., Praz,F. and Amor-Gueret,M. (1997) Characterization of a new BLM mutation associated with a topoisomerase II alpha defect in a patient with Bloom's syndrome. *Hum. Mol. Genet.*, **6**, 1427–1434.
- Gajiwala,K.S. and Burley,S.K. (2000) Winged helix proteins. *Curr. Opin. Struct. Biol.*, **10**, 110–116.
- Gangloff,S., McDonald,J.P., Bendixen,C., Arthur,L. and Rothstein,R. (1994) The yeast type I topoisomerase Top3 interacts with Sgs1, a DNA helicase homolog: a potential eukaryotic reverse gyrase. *Mol. Cell Biol.*, **14**, 8391–8398.
- Gorbalenya,A.E. and Koonin,E.V. (1993) Helicases: amino acid sequence comparisons and structure–function relationships. *Curr. Opin. Struct. Biol.*, **3**, 419–429.
- Hanada,K., Ukita,T., Kohno,Y., Saito,K., Kato,J. and Ikeda,H. (1997) RecQ DNA helicase is a suppressor of illegitimate recombination in *Escherichia coli*. *Proc. Natl Acad. Sci. USA*, **94**, 3860–3865.
- Harmon,F.G., DiGate,R.J. and Kowalczykowski,S.C. (1999) RecQ helicase and topoisomerase III comprise a novel DNA strand passage function: a conserved mechanism for control of DNA recombination. *Mol. Cell*, **3**, 611–620.
- Harmon,F.G. and Kowalczykowski,S.C. (1998) RecQ helicase, in concert with RecA and SSB proteins, initiates and disrupts DNA recombination. *Genes Dev.*, **12**, 1134–1144.
- Harmon,F.G. and Kowalczykowski,S.C. (2001) Biochemical characterization of the DNA helicase activity of the *Escherichia coli* RecQ helicase. *J. Biol. Chem.*, **276**, 232–243.
- Holm,L. and Sander,C. (1993) Protein structure comparison by alignment of distance matrices. *J. Mol. Biol.*, **233**, 123–138.
- Hunt,J.B., Neece,S.H., Schachman,H.K. and Ginsburg,A. (1984) Mercurial-promoted Zn<sup>2+</sup> release from *Escherichia coli* aspartate transcarbamoylase. *J. Biol. Chem.*, **259**, 14793–14803.
- Janscak,P., Garcia,P.L., Hamburger,F., Makuta,Y., Shiraishi,K., Imai,Y., Ikeda,H. and Bickle,T.A. (2003) Characterization and mutational analysis of the RecQ core of the Bloom syndrome protein. *J. Mol. Biol.*, **330**, 29–42.
- Jones,T.A., Zou,J.Y., Cowan,S.W. and Kjeldgaard,M. (1991) Improved methods for building protein models in electron density maps and the location of errors in these models. *Acta Crystallogr. D*, **47**, 110–119.
- Kabsch,W. (1988) Evaluation of single-crystal X-ray diffraction from a position sensitive detector. *J. Appl. Crystallogr.*, **21**, 916–924.
- Karow,J.K., Newman,R.H., Freemont,P.S. and Hickson,I.D. (1999) Oligomeric ring structure of the Bloom's syndrome helicase. *Curr. Biol.*, **9**, 597–600.
- Karow,J.K., Wu,L. and Hickson,I.D. (2000) RecQ family helicases: roles in cancer and aging. *Curr. Opin. Genet. Dev.*, **10**, 32–38.
- Kawasaki,K., Maruyama,S., Nakayama,M., Matsumoto,K. and Shibata,T. (2002) *Drosophila melanogaster* RECQ5/QE DNA helicase: stimulation by GTP binding. *Nucleic Acids Res.*, **30**, 3682–3691.
- Kim,J.L., Morgenstern,K.A., Griffith,J.P., Dwyer,M.D., Thomson,J.A., Murcko,M.A., Lin,C. and Caron,P.R. (1998) Hepatitis C virus NS3 RNA helicase domain with a bound oligonucleotide: the crystal structure provides insights into the mode of unwinding. *Structure*, **6**, 89–100.
- Kitao,S., Shimamoto,A., Goto,M., Miller,R.W., Smithson,W.A., Lindor,N.M. and Furuichi,Y. (1999) Mutations in RECQL4 cause a subset of cases of Rothmund–Thomson syndrome. *Nat. Genet.*, **22**, 82–84.
- Korolev,S., Hsieh,J., Gauss,G.H., Lohman,T.M. and Waksman,G. (1997) Major domain swivelling revealed by the crystal structures of complexes of *E.coli* Rep helicase bound to single-stranded DNA and ADP. *Cell*, **90**, 635–647.
- Kowalczykowski,S.C., Dixon,D.A., Eggleston,A.K., Lauder,S.D. and Rehauer,W.M. (1994) Biochemistry of homologous recombination in *Escherichia coli*. *Microbiol. Rev.*, **58**, 401–465.
- Krishna,S.S., Majumdar,I. and Grishin,N.V. (2003) Structural classification of zinc fingers. *Nucleic Acids Res.*, **31**, 532–550.
- Lamzin,V.S. and Wilson,K.S. (1993) Automated refinement of protein models. *Acta Cryst. D*, **49**, 129–147.
- Leslie,A.G.W. (1992) Newsletter on Protein Crystallography No. 26, Daresbury Laboratory.
- Lima,C.D., Wang,J.C. and Mondragon,A. (1994) Three-dimensional structure of the 67K N-terminal fragment of *E. coli* DNA topoisomerase I. *Nature*, **367**, 138–146.
- Liu,L.F. and Wang,J.C. (1987) Supercoiling of the DNA template during transcription. *Proc. Natl Acad. Sci. USA*, **84**, 7024–7027.
- Liu,Z., Macias,M.J., Bottomley,M.J., Stier,G., Linge,J.P., Nilges,M., Bork,P. and Sattler,M. (1999) The three-dimensional structure of the HRDC domain and implications for the Werner and Bloom syndrome proteins. *Structure*, **7**, 1557–1566.
- Matsumoto,T., Imamura,O., Goto,M. and Furuichi,Y. (1998) Characterization of the nuclear localization sequence in the DNA helicase involved in Werner's syndrome. *Int. J. Mol. Med.*, **1**, 71–76.
- Matsumoto,T., Shimamoto,A., Goto,M. and Furuichi,Y. (1997) Impaired nuclear localization of defective DNA helicases in Werner's syndrome. *Nat. Genet.*, **16**, 335–336.
- Mondragon,A. and DiGate,R. (1999) The structure of *Escherichia coli* DNA topoisomerase III. *Struc. Fold Des.*, **7**, 1373–1383.
- Morozov,V., Mushegian,A.R., Koonin,E.V. and Bork,P. (1997) A putative nucleic acid-binding domain in Bloom's and Werner's syndrome helicases. *Trends Biochem. Sci.*, **22**, 417–418.

- Mullen, J.R., Kaliraman, V. and Brill, S.J. (2000) Bipartite structure of the Sgs1 DNA helicase in *Saccharomyces cerevisiae*. *Genetics*, **154**, 1101–1114.
- Mullen, J.R., Kaliraman, V., Ibrahim, S.S. and Brill, S.J. (2001) Requirement for three novel protein complexes in the absence of the Sgs1 DNA helicase in *Saccharomyces cerevisiae*. *Genetics*, **157**, 103–118.
- Murshudov, G.N., Vagin, A.A. and Dodson, E.J. (1997) Refinement of macromolecular structures by the maximum-likelihood method. *Acta Crystallogr. D*, **53**, 240–255.
- Nakayama, H., Nakayama, K., Nakayama, R., Irino, N., Nakayama, Y. and Hanawalt, P.C. (1984) Isolation and genetic characterization of a thymineless death-resistant mutant of *Escherichia coli* K12: identification of a new mutation (recQ1) that blocks the RecF recombination pathway. *Mol. Gen. Genet.*, **195**, 474–480.
- Navaza, J. (2001) Implementation of molecular replacement in AMoRe. *Acta Crystallogr. D*, **57**, 1367–1372.
- Nicholls, A., Sharp, K.A. and Honig, B. (1991) Protein folding and association: insights from the interfacial and thermodynamic properties of hydrocarbons. *Proteins*, **11**, 281–296.
- Oakley, T.J. and Hickson, I.D. (2002) Defending genome integrity during S-phase: putative roles for RecQ helicases and topoisomerase III. *DNA Repair (Amst.)*, **1**, 175–207.
- Onoda, F., Seki, M., Miyajima, A. and Enomoto, T. (2000) Elevation of sister chromatid exchange in *Saccharomyces cerevisiae* sgs1 disruptants and the relevance of the disruptants as a system to evaluate mutations in Bloom's syndrome gene. *Mutat. Res.*, **459**, 203–209.
- Otwinowski, Z. (1991) Isomorphous Refinement and Anomalous Scattering. *Proceedings of the CCP4 Study Weekend*, 80–86.
- Peter, B.J., Ullsperger, C., Hiasa, H., Marians, K.J. and Cozzarelli, N.R. (1998) The structure of supercoiled intermediates in DNA replication. *Cell*, **94**, 819–827.
- Riddles, P.W., Blakeley, R.L. and Zerner, B. (1983) Reassessment of Ellman's reagent. *Methods Enzymol.*, **91**, 49–60.
- Rodriguez, A.C. and Stock, D. (2002) Crystal structure of reverse gyrase: insights into the positive supercoiling of DNA. *EMBO J.*, **21**, 418–426.
- Rong, S.B., Valiaho, J. and Vihinen, M. (2000) Structural basis of Bloom syndrome (BS) causing mutations in the BLM helicase domain. *Mol. Med.*, **6**, 155–164.
- Schneider, T.R. and Sheldrick, G.M. (2002) Substructure solution with SHELXD. *Acta Crystallogr. D*, **58**, 1772–1779.
- Schultz, S.C., Shields, G.C. and Steitz, T.A. (1991) Crystal structure of a CAP-DNA complex: the DNA is bent by 90 degrees. *Science*, **253**, 1001–1007.
- Singleton, M.R., Scaife, S. and Wigley, D.B. (2001) Structural analysis of DNA replication fork reversal by RecG. *Cell*, **107**, 79–89.
- Story, R.M., Li, H. and Abelson, J.N. (2001) Crystal structure of a DEAD box protein from the hyperthermophile *Methanococcus jannaschii*. *Proc. Natl Acad. Sci. USA*, **98**, 1465–1470.
- Subramanya, H.S., Bird, L.E., Brannigan, J.A. and Wigley, D.B. (1996) Crystal structure of a DExx box DNA helicase. *Nature*, **384**, 379–383.
- Ui, A., Satoh, Y., Onoda, F., Miyajima, A., Seki, M. and Enomoto, T. (2001) The N-terminal region of Sgs1, which interacts with Top3, is required for complementation of MMS sensitivity and suppression of hyper-recombination in sgs1 disruptants. *Mol. Genet. Genomics*, **265**, 837–850.
- Umez, K., Nakayama, K. and Nakayama, H. (1990) *Escherichia coli* RecQ protein is a DNA helicase. *Proc. Natl Acad. Sci. USA*, **87**, 5363–5367.
- Van Duyne, G.D., Standaert, R.F., Karplus, P.A., Schreiber, S.L. and Clardy, J. (1993) Atomic structures of the human immunophilin FKBP-12 complexes with FK506 and rapamycin. *J. Mol. Biol.*, **229**, 105–124.
- Velankar, S.S., Soutanas, P., Dillingham, M.S., Subramanya, H.S. and Wigley, D.B. (1999) Crystal structures of complexes of PcrA DNA helicase with a DNA substrate indicate an inchworm mechanism. *Cell*, **97**, 75–84.
- Wang, J.C. (2002) Cellular roles of DNA topoisomerases: a molecular perspective. *Nat. Rev. Mol. Cell Biol.*, **3**, 430–440.
- Whitby, M.C. and Lloyd, R.G. (1998) Targeting Holliday junctions by the RecG branch migration protein of *Escherichia coli*. *J. Biol. Chem.*, **273**, 19729–19739.
- Wu, L. and Hickson, I.D. (2001) RecQ helicases and topoisomerases: components of a conserved complex for the regulation of genetic recombination. *Cell. Mol. Life Sci.*, **58**, 894–901.
- Wu, L. and Hickson, I.D. (2002) RecQ helicases and cellular responses to DNA damage. *Mutat. Res.*, **509**, 35–47.
- Xu, H.Q., Deprez, E., Zhang, A.H., Tauc, P., Ladjimi, M.M., Brochon, J.-C., Auclair, C. and Xi, X.G. (2003) The *Escherichia coli* RecQ helicase functions as a monomer. *J. Biol. Chem.*, (published on line, June 12, 2003).
- Yao, N., Hesson, T., Cable, M., Hong, Z., Kwong, A.D., Le, H.V. and Weber, P.C. (1997) Structure of the hepatitis C virus RNA helicase domain. *Nat. Struct. Biol.*, **4**, 463–467.
- Yu, C.E. et al. (1996) Positional cloning of the Werner's syndrome gene. *Science*, **272**, 258–262.

Received June 23, 2003; revised July 28, 2003;  
accepted August 12, 2003